

A New Laser Cooling Concept for Molecular Translational Motion

C. H. Raymond Ooi*, Karl Peter Marzlin† and Jürgen Audretsch‡
*Fachbereich Physik der Universität Konstanz, Fach M674, D-78457
Konstanz, Germany*

We propose a laser cooling concept for the translational motion of molecules which does not require repeated spontaneous emission by each molecule. The cooling works by repetition of three main steps: velocity selection of a narrow momentum width, deceleration of velocity selected molecules and accumulation of the decelerated molecules by an irreversible process, namely by single spontaneous emission. We develop a cooling model which enables analytical description of the transient populations and entropies for the total molecular system, the center of mass degree of freedom and the internal degrees of freedom. Simulation shows that the cooling process can reduce a large momentum width to a final width which in principle can be arbitrarily small. Center of mass entropy is reduced while the internal entropy is increased after cooling. We show that translational cooling can occur during coherent laser interactions. The entropies change in consistency with the Araki-Lieb inequality.

I. INTRODUCTION

The existing laser cooling schemes for atoms have been successfully based on the concept of a repeated process of optical pumping up followed by spontaneous emission. In molecules, there are additional motional degrees of freedom, namely the vibrational and rotational motions in addition to the center of mass translational motion. This creates two characteristics in molecules which are absent in atoms. First, the optical spontaneous emission (fluorescence) will inevitably repopulate more than one state. This makes existing cooling schemes unapplicable to molecules. Second, the existence of additional quantum states associated with the vibrational and rotational motions creates new Hilbert spaces which are sufficiently large as entropy sinks. Our cooling concept circumvents the former and utilizes the latter to cool the translational motion of a molecular gas.

Laser cooling of translational motion of molecules seems to be a formidable challenge due to the difficulty of maintaining a closed optical pumping cycle. Some schemes have been proposed [1,2] which rely directly on incoherent processes for dissipation. Closed cycles in far-infrared and microwave regimes are available but may not be favorable due to their low spontaneous emission rates. For molecules, the pumping into the trapping state is not as efficient as for atoms [3,4] since fluorescence from the excited electronic state will populate other molecular levels and leads to inefficient returning to the original ground state. Thus, a closed *optical* pumping cycle which involves *repeated* spontaneous emissions cannot be simply established in molecules for continuous removal of the translational kinetic energy and entropy. However, closed optical pumping cycles based solely on coherent processes can easily be realized using lasers which are far detuned from an excited state. Using counter-intuitive pulses of STIRAP (*Stimulated Raman Adiabatic Passage*), a closed pumping cycle can be obtained even with zero detuned pulses without populating the excited state [6].

II. COOLING CONCEPT

In this paper, we propose a laser cooling concept for the translational motion of molecules. We describe the cooling process with an analytical model and demonstrate the cooling results by numerical simulations. The cooling process is based on the repetition of a cooling cycle, each composed of three different physical steps: 1) velocity selection, 2) deceleration and 3) accumulation. We refer to the molecules as a *total system* (subscript 'tot') with two subsystems:

*ooi@spock.physik.uni-konstanz.de

†Peter.Marzlin@uni-konstanz.de

‡Juergen.Audretsch@uni-konstanz.de

the electronic, vibrational and rotational states as the *internal* degree of freedom (subscript ‘I’) and the molecular center of mass as the *external* degree of freedom (subscript ‘cm’). The velocity selection and deceleration involve 4 internal levels, namely 3 ground states $|g0, \pm\rangle$ corresponding to the states with magnetic quantum number $M = 0, \pm 1$ and an excited state $|e\rangle$ ($M = 0$) (Fig.1a and 1b). The states $|e\rangle, |g0\rangle$ and $|g+\rangle$ are used for velocity selection while the deceleration are based on the states $|e\rangle, |g-\rangle$ and $|g+\rangle$. For convenience, we may refer to $|g0\rangle$ and $|g\pm\rangle$ as *initial state* and *Raman states* respectively. We assume that initially $|g\pm\rangle$ and $|e\rangle$ are empty, and only $|g0\rangle$ is populated with large momentum width.

In the *first step*, the velocity selection is performed (see Fig.1a and 2a). A fraction of molecules with narrow momentum width and mean momentum P is selected from the population in state $|g0\rangle$ and transferred to an empty state $|g+\rangle$ using a π -pulse, without populating the excited state. This step is essentially the same as described in Ref.[4,5] except that here we use orthogonal *lin* - σ^+ lasers instead of counter propagating $\sigma^+ - \sigma^-$ lasers, since the dipole moment between states $|g0\rangle$ and $|e\rangle$ is aligned along the σ^+ polarized laser axis.

In the *second step* (see Fig.1b and 2b), the selected molecules are decelerated using a coherent process. Various efficient deceleration techniques can be applied [7]. Here, we choose the technique of repeated population inversions between the Raman states $|g+\rangle$ and $|g-\rangle$ in order to maintain all-optical cooling. This deceleration technique uses STIRAP processes [6] which have been shown to be highly efficient in molecules [8] and in atom interferometry [9]. In this step, the internal populations are repeatedly inverted between $|g+\rangle$ and $|g-\rangle$. Each inversion is a *substep* of step 2, which is accomplished by reversing the directions and the counter-intuitive sequence of a pair of counter propagating σ^+ and σ^- polarized pulses. Each pair of the STIRAP pulse provides about $2\hbar k$ of photon momentum kick to decelerate the molecules. Thus, the population with a mean momentum P will require a number of $P/2\hbar k$ STIRAP inversions to reduce the mean momentum P towards zero. In the end of this step, we have a fraction of molecules with the translational energy close to zero.

We want to repeat steps 1 and 2 to accumulate the populations with narrow momentum width around zero momentum. Since steps 1 and 2 are coherent processes, subsequent repetition of these steps would not lead to net cooling because the next STIRAP process would accelerate the molecules out of zero mean momentum. The Raman states must be emptied before the next deceleration cycle starts. We achieve this with an irreversible process in the *third step* (see Fig.1c and 2c). The cooled and decelerated molecules are rapidly transferred from the Raman states to a decaying state $|d\rangle$, which is typically an excited electronic state. Subsequent spontaneous emissions populate the many accumulation states $\{|acc\rangle\}$. The molecules in states $\{|acc\rangle\}$ are decoupled from the laser beams. It is the irreversibility of the spontaneous emission which enables repeated accumulation of the molecules with narrow momentum slices and zero mean momentum from each cooling cycle as steps 1, 2 and 3 are repeated.

Each *cooling cycle* which is composed of a sequence of the three steps described above, begins with the velocity selection of a new slice of narrow momentum width. The whole cooling process involves the repetition of the cooling cycle. We point out that the equivalent temperature of the molecules after the process corresponds to the velocity selected momentum width, which can be well below the recoil limit.

The main difficulty to laser cool molecules by repeated spontaneous emissions in the optical regime is due to the fluorescence decay from an excited electronic state to many rotational-vibrational states of the ground electronic state. After a spontaneous emission, the molecules have a high probability of not returning to the original state. Thus, the molecules decay to a state which is off-resonant with the pumping laser before their momenta are reduced by the laser photons. In our cooling scheme, the momentum and kinetic energy of each molecule are reduced towards zero by deceleration (step 2) *before* undergoing a *single spontaneous emission* process in the end of a cooling cycle. Thus, each cooling cycle can be viewed as a complete cooling process for a particular fraction of molecules. This cooling scheme circumvents the requirement of repeated spontaneous emissions for each molecule to obtain cooling. It is this unique feature which makes translational laser cooling of molecules possible.

III. INITIAL STATE AND DENSITY MATRICES

We assume that initially the internal state is pure and uncorrelated to the center of mass momentum state. Only the internal state $|g0\rangle$ is occupied. If the molecular gas is in thermal equilibrium at temperature T , the center of mass subsystem is in the *Gibbs state* [11] and the initial total density operator is written as

$$\hat{\rho}_{tot}(0) = \hat{\rho}_I(0) \otimes \hat{\rho}_{cm}(0) = |g0\rangle\langle g0| \otimes \sum_P W(P)|P\rangle\langle P| \quad (1)$$

where $W(P) = \frac{1}{Z}e^{-P^2/\sigma^2}$ is the statistical weight, $Z = \sum_P e^{-P^2/\sigma^2}$ is the partition function and $\sigma = \sqrt{2Mk_B T}$ is the initial momentum width.

We also assume that the molecular gas is sufficiently dilute so that rethermalization by molecular collisions is negligible. Also, we suppose that the gas is homogeneously distributed in space within a confinement of fixed volume and spatial density. On one hand the gas is coupled to lasers, while on the other hand it forms an open system whereby it can exchange entropy with the outside environment.

The quantum dynamical evolution of the molecules in each cooling step and throughout the cooling process can be modeled analytically by using the density matrix elements. This enables convenient evaluation of the internal and center of mass subsystems probability distributions and the corresponding entropies, which allow us to work out the dynamics and the cooling efficiency. The density matrices of the total system, internal subsystem and center of mass subsystem in internal basis $\{|a\rangle\}$ and center of mass momentum basis $\{|P\rangle\}$, are defined respectively as

$$\hat{\rho}_{tot}(t) \doteq \sum_{a,b} \sum_{P,P'} \rho_{ab}(P,P',t) |a,P\rangle \langle b,P'| \quad (2)$$

$$\hat{\rho}_I(t) \doteq Tr_{cm}\{\hat{\rho}_{tot}(t)\} = \sum_{a,b} |a\rangle \langle b| \sum_P \rho_{ab}(P,P,t) \quad (3)$$

$$\hat{\rho}_{cm}(t) \doteq Tr_I\{\hat{\rho}_{tot}(t)\} = \sum_{P,P'} |P\rangle \langle P'| \sum_a \rho_{aa}(P,P',t) \quad (4)$$

where $\rho_{ab}(P,P',t) \doteq \langle a,P | \hat{\rho}_{tot}(t) | b,P' \rangle$ are the total system density matrix elements, $a, b \in \{e, g0, g\pm, d, \{acc_j\}\}$ the internal states and $\{P, P'\}$ the center of mass momenta along $\sigma\pm$ polarized lasers axis (defined as z -axis).

The time evolution dynamics of the total system in step 1 and step 2 are formally described by the 3-level Bloch equations [3]. In step 1 the total system states are $|g0, P\rangle$, $|e, P\rangle$ and $|g+, P - \hbar k\rangle$. A STIRAP inversion from $|g+\rangle$ to $|g-\rangle$ in step 2 involves the momentum family of states $|g+, P + \hbar k\rangle$, $|e, P\rangle$ and $|g-, P - \hbar k\rangle$. Due to the reversal of the pulses during subsequent inversion from $|g-\rangle$ to $|g+\rangle$, the family of states becomes $|g-, P - \hbar k\rangle$, $|e, P - 2\hbar k\rangle$ and $|g+, P - 3\hbar k\rangle$. With the high populations transfer efficiency of STIRAP, the center of mass coherences in the populations, for example $\langle g+, P - \hbar k | \hat{\rho}_{tot}(t) | g+, P - 3\hbar k \rangle$, are negligibly small. We start with populations in the internal state $|g0\rangle$ and the center of mass Gibbs state with no coherences in momentum basis. So, the only non vanishing matrix elements are $\rho_{00}(P, P, 0)$. The processes of a velocity selection, a STIRAP inversion and a spontaneous emission do not create center of mass coherences. Therefore, the populations remain diagonal in momentum basis throughout the cooling process: $\rho_{aa}(P, P', t) = \rho_{aa}(P, P, t) \delta_{P,P'}$.

On the other hand, transitions between different internal states are accompanied by momentum recoil. Thus, the matrix elements between different internal states ($a \neq b$) are non vanishing only for the center of mass coherences $P \neq P' : \rho_{ab}(P, P', t) \neq 0$ and $\rho_{ab}(P, P, t) = 0$. Accordingly, Eqs. (3) and (4) reduce to

$$\hat{\rho}_I(t) = \sum_a C_a(t) |a\rangle \langle a| \quad (5)$$

$$\hat{\rho}_{cm}(t) = \sum_P f(P, t) |P\rangle \langle P| \quad (6)$$

where the internal and center of mass probability distributions $C_a(t)$ and $f(P, t)$ are respectively defined as

$$C_a(t) \doteq \sum_P \rho_{aa}(P, P, t) \quad (7)$$

$$f(P, t) \doteq \sum_a \rho_{aa}(P, P, t) \quad (8)$$

Thus, we only need to evaluate the diagonal density matrix elements $\rho_{aa}(P, P, t)$ in order to calculate the subsystem density matrices and the corresponding entropies.

IV. POPULATION DYNAMICS

Step 1 of N-th cooling cycle: To simplify the mathematics, we can model the velocity selected momentum distribution by a Gaussian function of a narrow width $\sigma_{vsel} (\ll \sigma)$. During step 1 of the N -th cooling cycle (subscript N:1), only the populations in the states $|g0\rangle$ and $|g+\rangle$ change with time and can be written analytically as the following:

$$\rho_{00}(P, P, t_1)_{N:1} = W(P) - \sum_{j=1}^{N-1} V_j(P) - V_N(P)h_1(t_1) \quad (9)$$

$$\rho_{++}(P, P, t_1)_{N:1} = h_1(t_1)W(P_N)e^{-(P+\alpha\hbar k_{N,+}-P_N)^2/\sigma_{vsel}^2} \quad (10)$$

where $0 \leq t_1 \leq \tau_1$. τ_1 is the duration of the population transfer in step 1. The function $h_1(t_1) = \sin^2 \pi t / 2\tau_1$ describes the time evolution of the populations. $V_j(P) \doteq W(P_j)e^{-(P-P_j)^2/\sigma_{vsel}^2}$ is the velocity selected distribution in the j -th ($j = 1 \dots N$) cooling cycle with mean momentum P_j , momentum width σ_{vsel} and mean population $W(P_j) \doteq \frac{1}{2}e^{-P_j^2/\sigma^2}$. $k_{N,+}$ is the σ^+ laser wavevector of the N -th cooling cycle and $\alpha = \text{sign}(P_j)$ determines the direction of the σ^+ laser to provide decelerating momentum kick.

The first term in Eq. (9) describes the initial populations distribution. The second term corresponds to the depleted populations after $N-1$ cooling cycles. The third term describes the transient population depletion in the N -th cooling cycle. In the end of step 1, the populations become

$$\rho_{00}(P, P, \tau_1)_{N:1} = W(P) - \sum_{j=1}^N V_j(P) \quad (11)$$

$$\rho_{++}(P, P, \tau_1)_{N:1} = W(P_N)e^{-(P+\alpha\hbar k_{N,+}-P_N)^2/\sigma_{vsel}^2} \quad (12)$$

Step 2 of N -th cooling cycle: There are many substeps within step 2. Only the populations in states $|g+\rangle$ and $|g-\rangle$ change with time during the n -th substep of step 2 in the N -th cooling cycle, according to

$$\rho_{aa}(P, P, t_2)_{N:2(n)} = h_2(t_2)W(P_N)e^{-(P+\alpha\hbar k_{N,+}+\alpha\Lambda_n-P_N)^2/\sigma_{vsel}^2} \quad (13)$$

$$\rho_{bb}(P, P, t_2)_{N:2(n)} = (1 - h_2(t_2))W(P_N)e^{-(P+\alpha\hbar k_{N,+}+\alpha\Lambda_{n-1}-P_N)^2/\sigma_{vsel}^2} \quad (14)$$

$$\rho_{++}(P, P, 0)_{N:2(1)} = \rho_{++}(P, P, \tau_1)_{N:1} \quad (15)$$

where $a = -, b = +$ for odd n (inversion from $|g+\rangle$ to $|g-\rangle$) and $a = +, b = -$ for even n . The time interval for every substep is $0 \leq t_2 \leq \tau_2$, each with the same duration τ_2 for complete inversion. $h_2(t_2) = \sin^2 \pi t / 2\tau_2$ describes the time evolution of the populations and $\Lambda_n \doteq \sum_{j=1}^n \hbar(k_{j+} + k_{j-}) \approx 2n\hbar k$ is the total amount of momentum transfer provided by n pairs of STIRAP pulses. The precise values of $k_{N,+}$, k_{j+} and k_{j-} are obtained via the two-photon Raman resonance condition. In the numerical simulations they are simply taken to be approximately equal to k without affecting the validity of the results.

The momentum width σ_{vsel} is unchanged throughout step 2. The number of deceleration cycles n_{\max} required to reduce the mean momentum from P_N to zero can be predicted through $\alpha\hbar k_{N,+} + \alpha\Lambda_n - P_N \approx \alpha\hbar k(1 + 2n_{\max}) - P_N \approx 0$, which gives

$$1 \leq n \leq (n_{\max} = \frac{P_N}{2\alpha\hbar k} - \frac{1}{2}). \quad (16)$$

In the end of step 2, the populations become

$$\rho_{aa}(P, P, \tau_2)_{N:2(n_{\max})} \approx W(P_N)e^{-P^2/\sigma_{vsel}^2} \quad (17)$$

Step 3 of N -th cooling cycle: After step 2, if the cooled populations from the Raman states $|g\pm\rangle$ are transferred rapidly to the decaying state $|d\rangle$ with a short π -pulse, the process is essentially unitary due to negligible spontaneous emissions from $|d\rangle$. Furthermore, if the laser is orthogonal to the z -direction, no momentum kick is imparted in z -direction. This enables the replacement $\rho_{dd}(P, P, 0)_{N:3} \approx \rho_{aa}(P, P, \tau_2)_{N:2(n_{\max})}$ as initial population, setting $\rho_{\pm\pm}(P, P, t_3)_{N:3} = 0$ and disregarding the dynamics of the π -pulse. The population in $|d\rangle$ decay to many vibrational-rotational levels in the ground electronic state. Assuming that only a small branching ratio of the population from $|d\rangle$ decays back to $|g\pm\rangle$, the time evolution of the populations in step 3 is simply due to the spontaneous decays from $|d\rangle$ to M number of accumulation states $\{|acc_j\rangle, j = 1 \dots M\}$ with the corresponding decay rates Γ_j . This is given by

$$\rho_{dd}(P, P, t_3)_{N:3} = \sum_{j=1}^M F_j e^{-\Gamma_j t_3} W(P_N) e^{-P^2/\sigma_{vsel}^2} \quad (18)$$

$$\rho_{acc_j}(P, P, t_3)_{N:3} = F_j \frac{\sigma_{vsel}}{\sigma_{acc}} e^{-P^2/\sigma_{acc}^2} \left\{ \sum_{j=1}^{N-1} W(P_j) + W(P_N)(1 - e^{-\Gamma_j t_3}) \right\} \quad (19)$$

where $0 \leq t_3 \leq \tau_3$ is the time interval for step 3, τ_3 is the duration for $|d\rangle$ to empty its populations to essentially zero (taken as $10/\Gamma_j$) and F_j is the Franck-Condon factor for level $|acc_j\rangle$ with $\sum_{j=1}^M F_j = 1$.

The first term in the curly bracket of Eq. (19) corresponds to the cumulative populations from the previous $N - 1$ cooling cycles. It is equal to the depleted populations from $|g0\rangle$ while the second term describes the transient increase in populations. The accumulated momentum width σ_{acc} is slightly larger than σ_{vsel} due to the small momentum spread (about $0.5\hbar k_a$) from a single spontaneous emission. The normalization factor $\frac{\sigma_{vsel}}{\sigma_{acc}}$ in Eq. (19) ensures that $Tr_{tot}\{\hat{\rho}_{tot}\} = 1$ and can be estimated by

$$\sigma_{acc}/\sigma_{vsel} \approx 1 + 0.5\hbar k_a/\sigma_{vsel} \quad (20)$$

where $k_a = (E_d - E_{acc})/\hbar c$.

V. ENTROPIES

The cooling effect is shown by the variation in the momentum probability distribution and the variations of the total, internal and center of mass von Neumann entropies [10]. From Eq. (1) the initial internal, center of mass and total entropies are respectively:

$$S_I(0) = 0 \quad (21)$$

$$S_{cm}(0) = -k_B \sum_P W(P) \ln W(P) \quad (22)$$

$$S_{tot}(0) = S_{cm}(0) \quad (23)$$

The expressions for internal and center of mass entropies are obtained from Eqs. (5)-(8) using $S_X(t) = Tr_X\{\hat{\rho}_X(t) \ln \hat{\rho}_X(t)\}$ where $X \in \{I, cm\}$, as follows:

$$S_I = -k_B \sum_a C_a \ln C_a \quad (24)$$

$$S_{cm} = -k_B \sum_P f(P) \ln f(P) \quad (25)$$

Equations (24) and (25) are valid for all times in all cooling steps and take a simple form because the reduced density matrices are diagonal (Eqs.(5) and (6)). The center of mass probability distributions for step 1, 2 and 3 of the N -th cooling cycle are given by:

$$f(P, t_1)_{N:1} = \sum_{a=0,+} \rho_{aa}(P, P, t_1)_{N:1} + \sum_j \rho_{acc_j}(P, P, \tau_3)_{(N-1):3} \quad (26)$$

$$f(P, t_2)_{N:2(n)} = \rho_{00}(P, P, \tau_1)_{N:1} + \sum_{a=+,-} \rho_{aa}(P, P, t_2)_{N:2(n)} + \sum_j \rho_{acc_j}(P, P, \tau_3)_{(N-1):3} \quad (27)$$

$$f(P, t_3)_{N:3} = \rho_{00}(P, P, \tau_1)_{N:1} + \rho_{dd}(P, P, t_3)_{N:3} + \sum_j \rho_{acc_j}(P, P, t_3)_{N:3} \quad (28)$$

Using $\int_{-\infty}^{\infty} e^{-(P-a)^2/\sigma_{vsel}^2} dP = \sigma_{vsel} \sqrt{\pi}$, we can show that $f(P)$ is normalized, $\int f(P) dP = 1$. Similarly, the internal probability distributions for step 1, 2 and 3 of the N -th cooling cycle are given by:

$$C_{0,+}(t_1)_{N:1} = \sum_P \rho_{00,++}(P, P, t_1)_{N:1} \quad (29)$$

$$C_{acc_j}(t_1)_{N:1} = \sum_P \rho_{acc_j}(P, P, \tau_3)_{(N-1):3}$$

$$C_0(t_2)_{N:2(n)} = \sum_P \rho_{00}(P, P, \tau_1)_{N:1}$$

$$C_{+,-}(t_2)_{N:2(n)} = \sum_P \rho_{+,-}(P, P, t_2)_{N:2(n)}$$

$$C_{acc_j}(t_2)_{N:2(n)} = \sum_P \rho_{acc_j}(P, P, \tau_3)_{(N-1):3} \quad (30)$$

$$\begin{aligned}
C_0(t_3)_{N:3} &= \sum_P \rho_{00}(P, P, \tau_1)_{N:1} \\
C_d(t_3)_{N:3} &= \sum_P \rho_{dd}(P, P, t_3)_{N:3} \\
C_{acc_j}(t_3)_{N:3} &= \sum_P \rho_{acc_j}(P, P, t_3)_{N:3}
\end{aligned} \tag{31}$$

The *total* density matrix in this step involves the basis states $|g0\rangle$, $|d\rangle$ and $\{|acc_j\rangle\}$. It is diagonal since these states are not coupled by laser. The evolution is characterized by free spontaneous emission from $|d\rangle$ to $\{|acc_j\rangle\}$. Thus, the time evolution of the total density matrix for step 3 can be written in a completely diagonal form

$$\hat{\rho}_{tot}(t_3)_{N:3} = \sum_P \{ \rho_{00}(P, P, \tau_1)_{N:1} |0, P\rangle \langle 0, P| + \sum_{a=d, \{acc_j\}} \rho_{aa}(P, P, t_3)_{N:3} |a, P\rangle \langle a, P| \} \tag{32}$$

with $Tr_{tot}\{\hat{\rho}_{tot,N}(t)\} = 1$.

The total entropy changes only during step 3 through the populations change in states $|d\rangle$ and $\{|acc_j\rangle\}$ and its time evolution in the N -th cooling cycle is given by

$$S_{tot}(t_3)_{N:3} = -k_B \sum_P \{ \rho_{00}(P, P, \tau_1)_{N:1} \ln \rho_{00}(P, P, \tau_1)_{N:1} + \sum_{a=d, \{acc_j\}} \rho_{aa}(P, P, t_3)_{N:3} \ln \rho_{aa}(P, P, t_3)_{N:3} \} \tag{33}$$

Throughout the coherent interactions of step 1 and step 2 in the N -th cooling cycle, the total entropy takes a constant value of $S_{tot}(\tau_3)_{(N-1):3}$.

VI. RESULTS AND DISCUSSIONS

Based on the model discussed above, we simulate the essential features of the cooling process. The typical variations of the internal populations distribution for each step in a cooling cycle is shown in Figs. 2. In each cooling cycle, a fraction of molecules with a narrow momentum width are depleted from the state $|g0\rangle$ by velocity selection (Fig. 2a), slowed towards zero mean momentum via repeated inversion by STIRAP (Fig. 2b) and dumped irreversibly into the accumulation states (Fig. 2c).

We give the overall results of the cooling process first and discuss the details of the cooling mechanism later. The cooling effect is shown by the narrowing of the momentum probability distribution $f(P)$, which evolves from a large momentum width (about $30\hbar k$) into a narrow momentum width (about $2\hbar k$) with zero mean momentum (Fig. 5). The main interest of this paper is the center of mass entropy S_{cm} which is found to decrease after the cooling process (Fig. 4a), in particular during velocity selection and deceleration since these steps move a fraction of the populations closer to zero momentum. This is the sign of cooling in the molecular translational degree of freedom. The coherent processes of steps 1 and 2 contribute substantially to the reduction of S_{cm} , from the maximum entropy of Gibbs state to the final populations with narrow momentum width. Throughout the cooling, the internal entropy S_I increases (Fig. 4a). Within each cooling cycle, the laser fields have created correlations between internal and center of mass momentum states, thus transferring the entropy from the center of mass to the internal subsystems by reducing the center of mass state dispersion while increasing the internal state dispersion. Indefinite repetition of the center of mass cooling effect is possible through the irreversible process of step 3.

We proceed to elaborate on the detailed features of the entropy variations in each cooling cycle with regard to the populations of the internal and center of mass states. During velocity selection, the extraction of a narrow slice of momentum from $|g0\rangle$ leads to distortion in the momentum distribution. One $\hbar k$ of momentum kick on the velocity selected population leads to a narrower overall momentum distribution and to the reduction of S_{cm} (Fig. 3a). At the same time, S_I increases (Fig. 3b) because an additional internal state $|g+\rangle$ is increasingly populated.

In the deceleration step, S_{cm} is reduced in each substep (Fig. 3a) by repeated momentum kicks which push the selected populations closer to zero mean momentum. Entanglement of the center of mass momentum states in each STIRAP process increases the population dispersion of the center of mass states. This explains the transient increase in S_{cm} , which is less than the overall reduction of S_{cm} in one STIRAP process. During the first STIRAP process in step 2, this transient increase is not observed because it is quenched by the rapid reduction of S_{cm} . The first STIRAP process reduces S_{cm} more than the subsequent ones. This quantitative difference is due to the nonlinear dependence of the entropy on the momentum distribution. However, S_I oscillates above a constant value (Fig. 3b). Each oscillation

corresponds to a substep, which is an inversion process by STIRAP and can be explained by the creation of adiabatic states through the entanglement of states $|g+\rangle$ and $|g-\rangle$. The entanglement involves the population of an additional internal state, thereby increasing S_I . After the completion of a STIRAP process, the entanglement disappears and S_I falls back to the value before the entanglement. Thus, the value of S_I before and after step 2 are the same.

The total entropy S_{tot} is constant throughout steps 1 and 2 but changes only during step 3 (Fig. 3c). This shows that unitary evolution can reduce the center of mass entropy despite the invariance of the total entropy. In other words, coherent interaction alone is able to cool the center of mass subsystem at the expense of heating the internal subsystem. However, the cooling cannot be repeated unless an irreversible process is introduced as part of the cooling cycle, which is step 3. In step 3, the slight increase in S_{cm} due to momentum spread from one spontaneous emission is smaller than the decrease in S_{cm} in steps 1 and 2 (Fig. 3a). This leads to the overall reduction of S_{cm} in each cooling cycle. In fact, it is the coherent process of steps 1 and 2 instead of the spontaneous emission, which substantially reduces S_{cm} . This is an essential point, as it indicates that *coherent process can lead to substantial change in the subsystem entropy*. The important role of the single spontaneous emission is to *irreversibly accumulate* the translationally cooled populations. We note that this accumulation role can also be realized if the cooled populations in each cooling cycle are coherently transferred to different internal $|acc\rangle$ states. For this, the number of $|acc\rangle$ states has to be more than the number of cooling cycles and multi-frequency lasers resonant with all the $|acc\rangle$ states would be required. In this case, the whole cooling process is coherent and *no spontaneous emission* is required. Then, both translational and internal cooling cannot be achieved simultaneously. Translational cooling must be accompanied by internal heating, or vice versa. Thus, coherent cooling of translational motion is not a conceptual impossibility but rather a practical one, at least at the present moment.

The entropy variations for a *single* $|acc\rangle$ state and *multi* $|acc\rangle$ states are shown in Fig. 3b and Fig. 3c (we use 10 $|acc\rangle$ states with logarithmic Franck-Condon factors and a fixed decay rate). With single $|acc\rangle$ state, S_I reduces during step 3 of the second cooling cycle because the number of internally populated states reduces from three populated states ($|g0\rangle, |g\pm\rangle, |acc\rangle$) to two states ($|g0\rangle, |acc\rangle$) (Fig. 3b). The center of mass entropy S_{cm} is unaffected by the number of $|acc\rangle$ states (Fig. 3a). However, the internal entropy S_I increases with more $|acc\rangle$ states since the number of populated internal states increases (Fig. 3b). It is interesting to observe that the increase in S_I from populating 10 internal states (in step 3) is still smaller than the increase in S_I from velocity selection (step 1). This is because entropy is not simply a measure of the number of occupied states, but also depends on the relative populations among the states.

The internal and center of mass entropies fluctuate throughout the cooling process (Fig. 4a). As the momentum width of the populations shrinks towards a narrow velocity selected width in the cooling process, the S_{cm} reduces from the maximum entropy state towards zero. The small residual populations in the right and left wings of the narrow peak (Fig. 5) is due to inefficient velocity selection with Gaussian momentum profile. In practice, a more efficient pulse shape can be tailored to selectively transfer the narrow populations as close to a square momentum profile as possible. This would bring the final S_{cm} closer to zero in the end of the cooling process. On overall, S_I increases in every cooling cycle due to the increase of the populations in the many $|acc\rangle$ states, thus changing from populating an internal state ($S_I = 0$) to populating multi internal $|acc\rangle$ states.

The total entropy S_{tot} before and after the cooling happen to be essentially the same (Fig. 4b). In fact, S_{tot} can increase or decrease due to the coupling of the total system to the environment. The total, internal and center of mass entropies satisfy the Araki-Lieb inequality [12], $|S_I - S_{cm}| \leq S_{tot} \leq S_I + S_{cm}$, as shown in Fig. 3c and 4b. Therefore, the cooling results are consistent with the general properties of quantum entropy. The non-negligible index of correlation $I_C = S_{cm} + S_I - S_{tot}$ [11] shows that the internal and center of mass subsystems are correlated by the laser interactions throughout the cooling process. However, after cooling the correlation is not maximum since S_{tot} is not zero and $S_{cm} \neq S_I$.

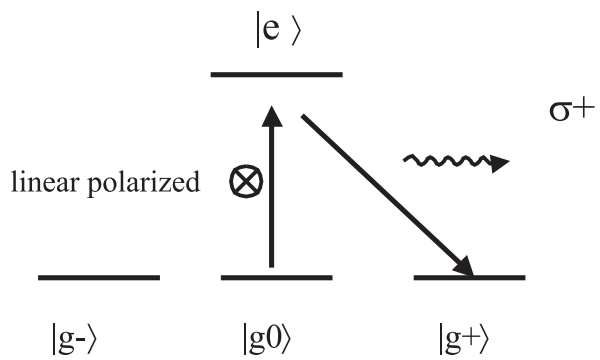
VII. CONCLUSIONS

We have developed a laser cooling concept for molecules based on the repetition of three steps: velocity selection, deceleration and accumulation by a single spontaneous emission per molecule. Each molecule need not undergo repeated spontaneous emissions to be translationally cooled. Numerical simulations have shown the reduction of the center of mass entropy by the cooling process as a molecular gas with an arbitrary large initial momentum width is cooled to a narrow width. We showed that the concept of cooling by a coherent process can work through the reduction of the center of mass entropy at the expense of increasing the internal entropy. The entropies in the cooling process satisfy the Araki-Lieb inequality. This cooling concept opens up a new possibility for laser cooling of molecules.

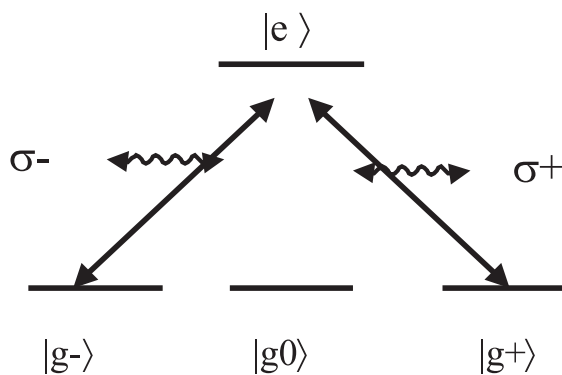
ACKNOWLEDGMENTS

We wish to thank Achim Peters, Dennis Weise and Thomas Konrad for discussions. Financial support by the Deutsche Forschungsgemeinschaft (Forschergruppe Quantengase) is gratefully acknowledged.

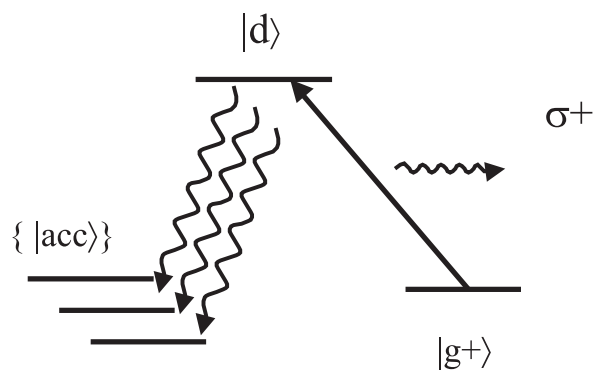
- [1] J. T. Bahns, W. C. Stwalley, and P. L. Gould, *J. Chem. Phys.* **104**, 9689 (1996).
- [2] V. Vuletic and S. Chu, *Phys. Rev. Lett.* **84**, 3787 (2000).
- [3] A. Aspect, E. Arimondo, R. Kaiser, N. Vansteenkiste and C. Cohen-Tannoudji, *J. Opt. Soc. Am. B* **6**, 2112 (1989).
- [4] Kasevich and S. Chu, *Phys. Rev. Lett.* **69**, 1741 (1992).
- [5] F. Harris, *Proc. IEEE* **66**, 51 (1978).
- [6] U. Gaubatz, P. Rudecki, S. Schiemann, and K. Bergmann, *J. Chem. Phys.* **92**, 5363 (1990); J. Oreg, F. T. Hioe, and J. H. Eberly, *Phys. Rev. A* **29**, 690 (1984).
- [7] H. L. Bethlem, G. Berden, and G. Meijer, *Phys. Rev. Lett.* **83**, 1558 (1999).
- [8] S. Schiemann, A. Kuhn, S. Steuerwald, and K. Bergmann, *Phys. Rev. Lett.* **71**, 3637 (1993); W. Suptitz, B. C. Duncan, and P. L. Gould, 1997, *J. Opt. Soc. Am. B* **14**, 1001 (1997).
- [9] M. Weitz, B. C. Young, and S. Chu, *Phys. Rev. Lett.* **73**, 2563 (1994).
- [10] J. von Neumann, *Gött. Nachr.* 273 (1927); A. Wehrl, *Rev. Mod. Phys.* **50**, 221 (1978).
- [11] G. Lindblad, *Non-Equilibrium Entropy and Irreversibility*, (Reidel, Dordrecht, 1983).
- [12] H. Araki and E. H. Lieb, *Commun. Math. Phys.* **18**, 160 (1970).



a)Step 1-Velocity selection



b)Step 2-Deceleration



c)Step 3-Accumulation

Figure 1

FIG. 1. Schematic diagrams for each cooling cycle composed of 3 sequential steps: a) narrow velocity width selection, b) deceleration of selected molecules and c) accumulation of decelerated and narrow momentum width molecules by a single spontaneous emission to one of the many accumulation states.

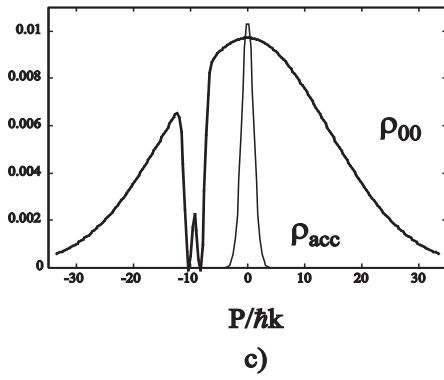
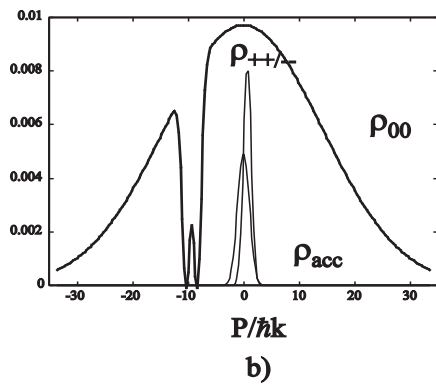
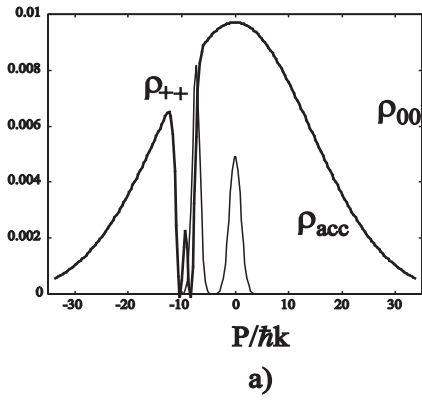
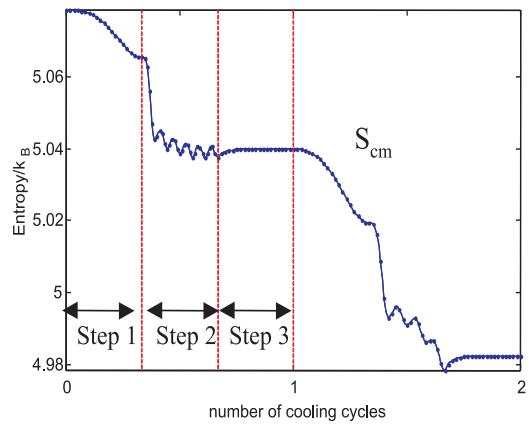
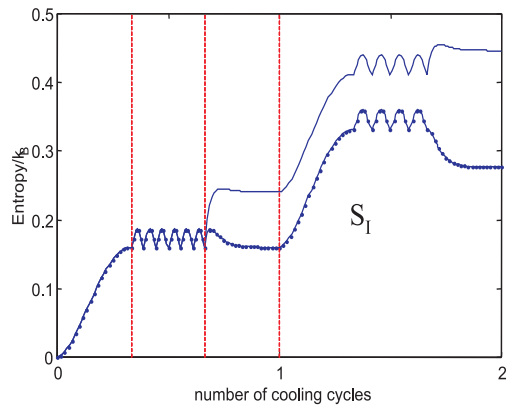


Figure 2

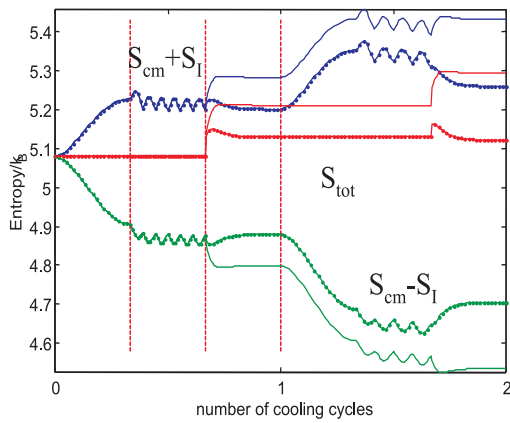
FIG. 2. Momentum distributions of the internal populations in a typical cooling cycle after the steps of: a) velocity selection, b) deceleration and c) accumulation.



a)



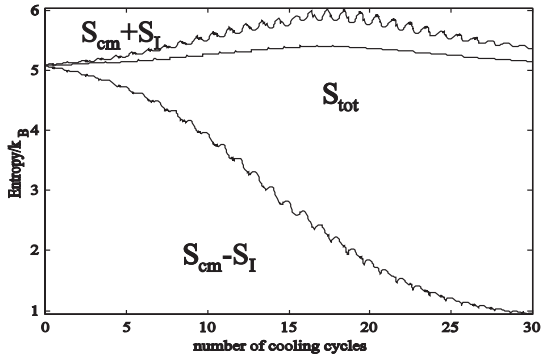
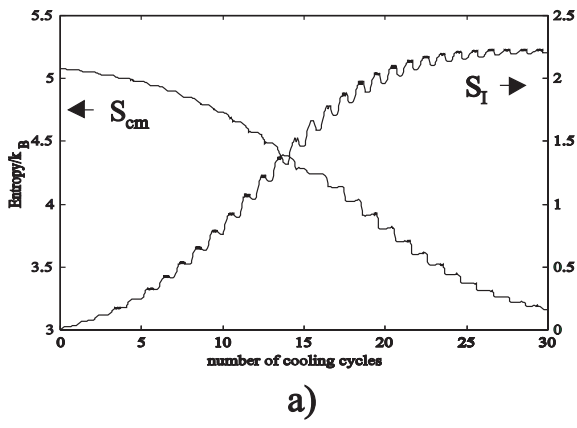
b)



c)

Figure 3

FIG. 3. Evolution of the a) center of mass entropy S_{cm} , b) internal entropy S_I , and c) total entropy S_{tot} as well as $S_{cm} \pm S_I$ throughout the first 2 cooling cycles with 1 accumulation state (line with dots) and 10 accumulation states (solid line). The abscissa of each cooling cycle is equally divided for the 3 cooling steps, each with different timescale.



b)
Figure 4

FIG. 4. Results after the whole cooling process with 10 accumulation states for a) S_{cm} and S_I , b) S_{tot} and $S_{cm} \pm S_I$.

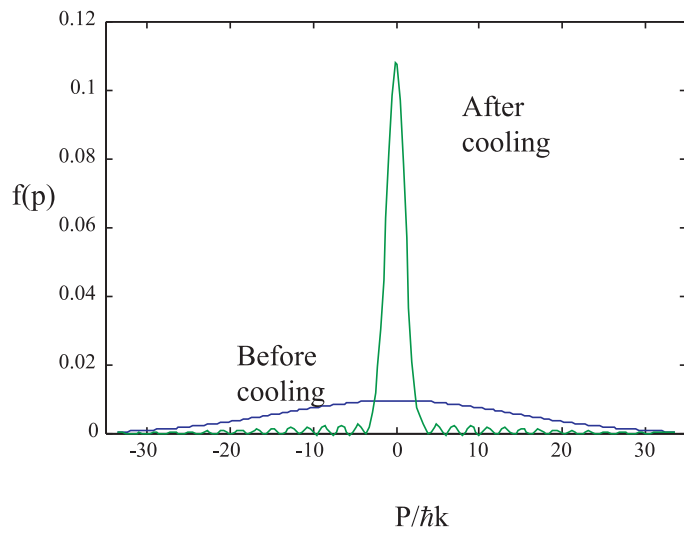


Figure 5

FIG. 5. Total momentum probability distribution $f(P)$ before and after the cooling process.